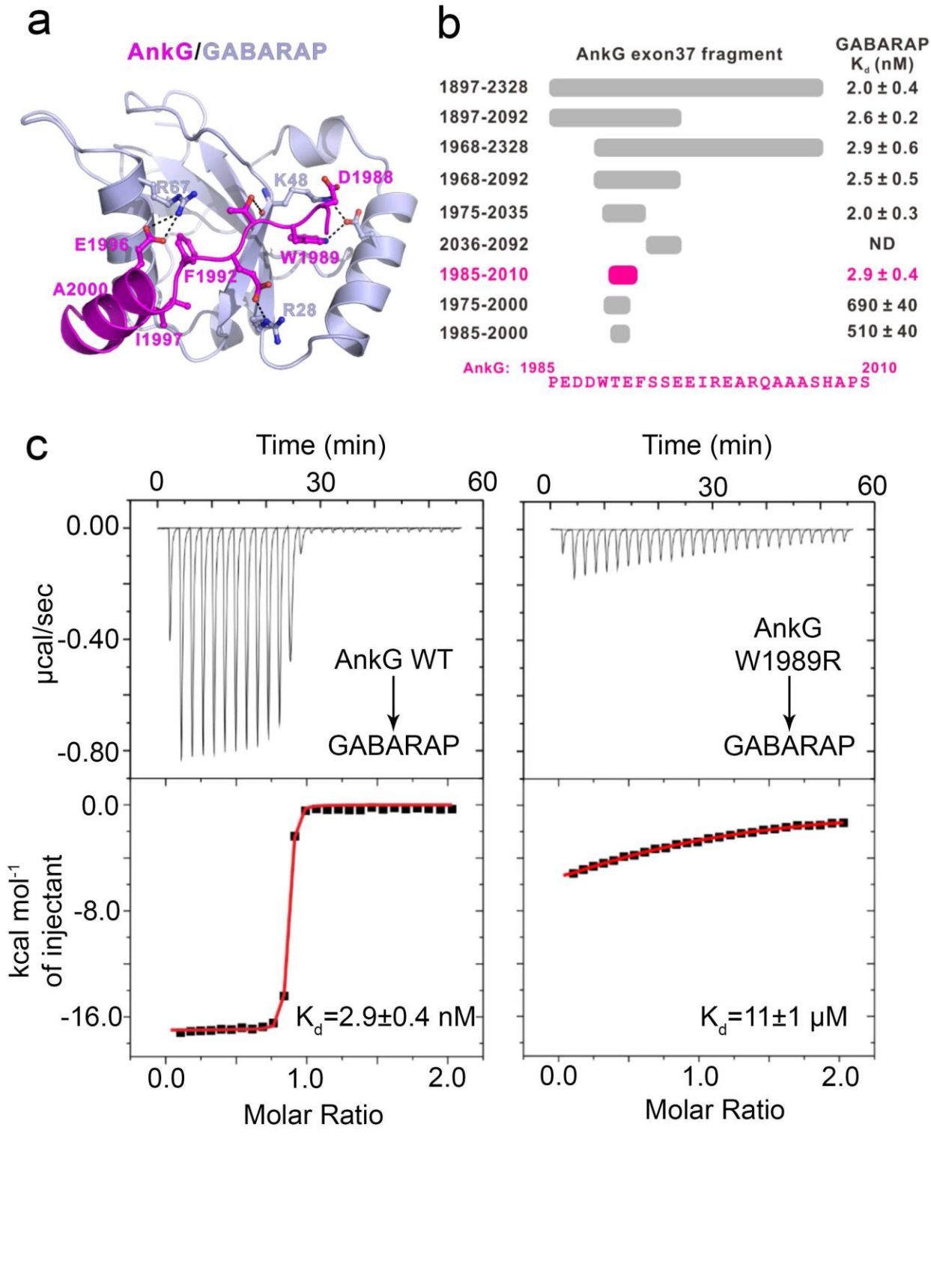
a
AnkG/GABARAP
R67
K48
D1988
E1996
W1989
F1992
A2000
R28
I1997
b
AnkG exon37 fragment
GABARAP
K_d (nM)
1897-2328
2.0 ± 0.4
1897-2092
2.6 ± 0.2
1968-2328
2.9 ± 0.6
1968-2092
2.5 ± 0.5
1975-2035
2.0 ± 0.3
2036-2092
ND
1985-2010
2.9 ± 0.4
1975-2000
690 ± 40
1985-2000
510 ± 40
AnkG: 1985
2010
PEDDWTEFSSEEIREARQAAASHAPS
c
Time (min)
0
30
60
0.00
-0.40
-0.80
µcal/sec
AnkG WT
GABARAP
AnkG
W1989R
GABARAP
0.0
-8.0
-16.0
kcal mol-1
of injectant
K_d=2.9±0.4 nM
K_d=11±1 µM
0.0
1.0
2.0
Molar Ratio

Supplementary Fig. 1: W1989 reside in ankyrin-G is necessary for high affinity binding to GABARAP.

(a) Ribbon representation of the ankyrin-G/GABARAP complex structure. Key residues critical for the binding are shown in the stick model. Salt bridges and hydrogen bonds are indicated with dashed lines. **(b)** Biochemical analysis of the complex formation between ankyrin-G and GABARAP. Isothermal Titration Calorimetry (ITC)-based mapping of the minimal region of the giant exon of ankyrin-G capable of binding to GABARAP. The minimal and complete fragment identified is highlighted in magenta, and the amino acid sequence of ankyrin-G 1985-2010 is listed at the bottom. “ND” denotes that the construct had no detectable binding to GABARAP. **(c)** ITC-derived binding curves of WT ankyrin-G and W1989R ankyrin-G to GABARAP.

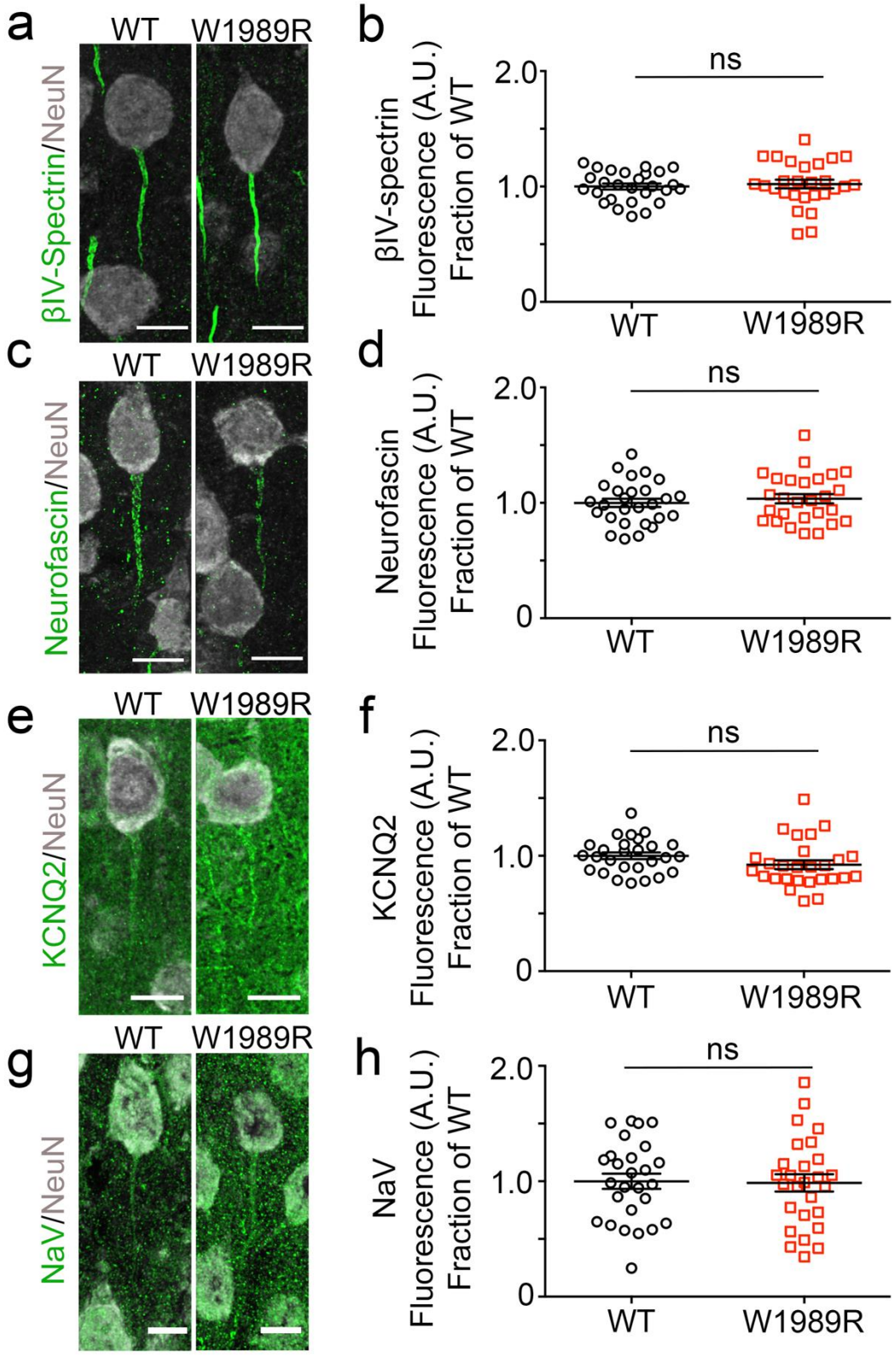
a
WT
W1989R
βIV-Spectrin/NeuN
b
βIV-spectrin
Fluorescence (A.U.)
Fraction of WT
ns
2.0
1.0
0
WT
W1989R
c
WT
W1989R
Neurofascin/NeuN
d
Neurofascin
Fluorescence (A.U.)
Fraction of WT
ns
2.0
1.0
0
WT
W1989R
e
WT
W1989R
KCNQ2/NeuN
f
KCNQ2
Fluorescence (A.U.)
Fraction of WT
ns
2.0
1.0
0
WT
W1989R
g
WT
W1989R
NaV/NeuN
h
NaV
Fluorescence (A.U.)
Fraction of WT
ns
2.0
1.0
0
WT
W1989R

Supplementary Fig. 2: W1989R 480 kDa ankyrin-G is capable of clustering all known ankyrin-G binding partners to the AIS.

(a) Representative images of the AIS of pyramidal neurons in layer II/III of the somatosensory cortex of P30 WT (left) and *Ank3* W1989R homozygous (right) mice. Coronal brain sections immunostained with βIV-spectrin (green) and NeuN (white). Scale bar: 10 µm. **(b)** Quantification of βIV-spectrin fluorescence intensity (a.u.) as fraction of WT between WT (black circles) and *Ank3* W1989R homozygous (red squares) mice. *t-test* P = 0.6375 (WT: 1 ± 0.03, N=3, n=27; W1989R: 1.02 ± 0.04, N=3, n=27). **(c)** Representative images of cortical pyramidal neuron AISs of P30 WT (left) and *Ank3* W1989R homozygous (right) mice immunostained with pan-neurofascin (green) and NeuN (white). Scale bar: 10 µm. **(d)** Quantification of neurofascin fluorescence intensity (a.u.) as fraction of WT between WT (black circles) and *Ank3* W1989R homozygous (red squares) mice. *t-test* P = 0.517 (WT: 1 ± 0.04, N=3, n=27; W1989R: 1.04 ± 0.04, N=3, n=27). **(e)** Representative images of cortical pyramidal neuron AISs of P30 WT (left) and *Ank3* W1989R homozygous (right) mice immunostained with KCNQ2 (green) and NeuN (white). Scale bar: 10 µm. **(f)** Quantification of KCNQ2 fluorescence intensity (a.u.) as fraction of WT between WT (black circles) and *Ank3* W1989R homozygous (red squares) mice. *t-test* P = 0.116 (WT: 1 ± 0.03, N=3, n=27; W1989R: 0.92 ± 0.03, N=3, n=27). **(g)** Representative images of cortical pyramidal neuron AISs of P30 WT (left) and *Ank3* W1989R homozygous (right) mice immunostained with pan-NaV (green) and NeuN (white). Scale bar: 10 µm. **(h)** Quantification of Nav fluorescence intensity (a.u.) as fraction of WT

between WT (black circles) and *Ank3* W1989R homozygous (red squares) mice. *t-test* P = 0.89 (WT: 1 ± 0.07, N=3, n=27; W1989R: 0.99 ± 0.07, N=3, n=27).

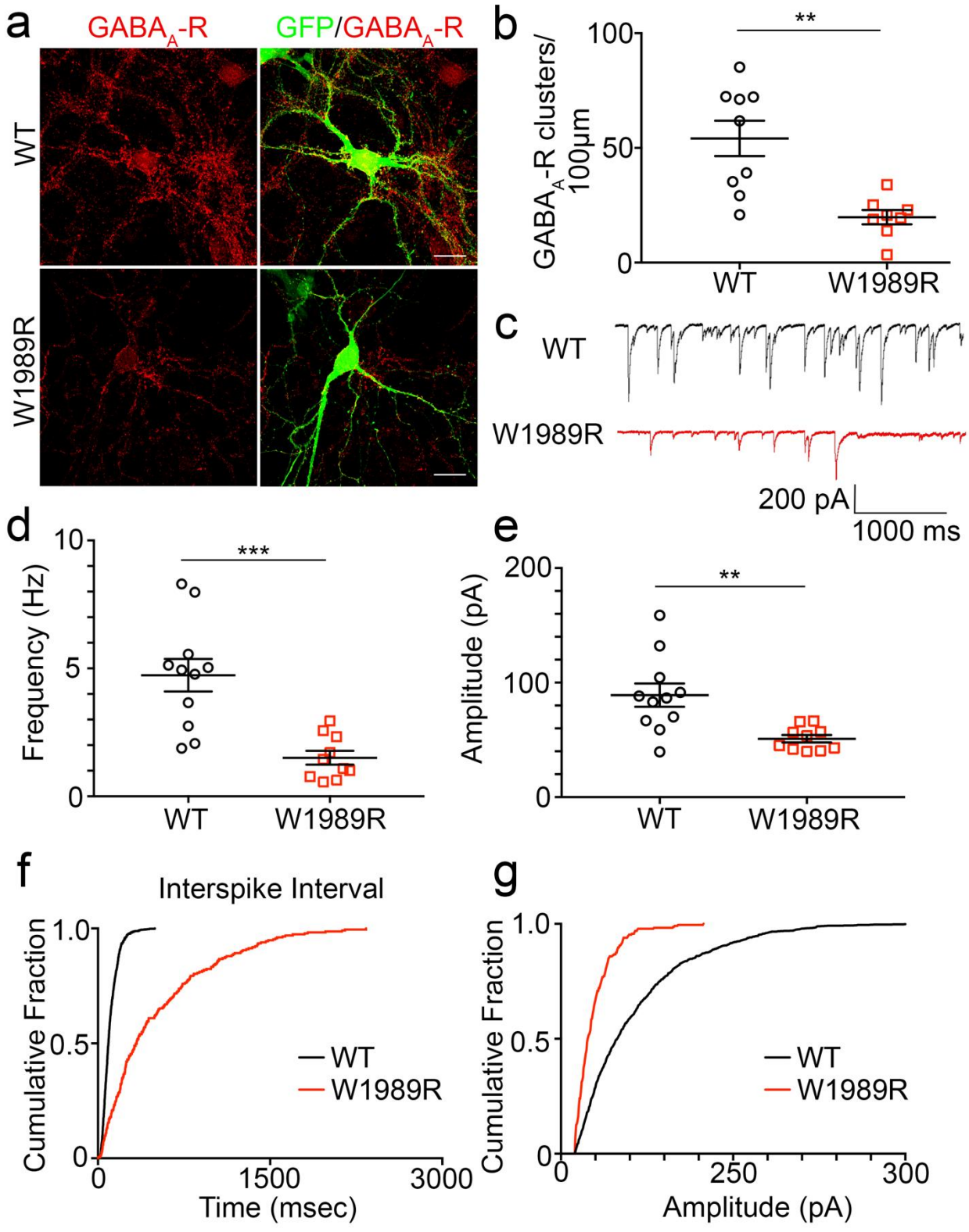
a
GABA$_A$-R
GFP/GABA$_A$-R
WT
W1989R
b
GABA$_A$-R clusters/ 100μm
100
50
0
**
WT
W1989R
c
WT
W1989R
200 pA
1000 ms
d
Frequency (Hz)
10
5
0
***
WT
W1989R
e
Amplitude (pA)
200
100
0
**
WT
W1989R
f
Interspike Interval
Cumulative Fraction
1.0
0.5
0
WT
W1989R
0
1500
3000
Time (msec)
g
Cumulative Fraction
1.0
0.5
0
WT
W1989R
0
250
300
Amplitude (pA)

Supplementary Fig. 3: Loss of pre- and post-synaptic GABAergic synapses in *Ank3* W1989R CA1 hippocampal neurons.

(a) Representative images of dissociated hippocampal cultured neurons at 21 DIV from WT (top) and *Ank3* W1989R homozygous (bottom) mice. Soluble GFP shown in green and immunostaining for $GABA_A$ receptor β2-3 subunit shown in red. Scale bar: 20 µm. **(b)** Quantification of the total number of $GABA_A$ receptor clusters per 100 µm per neuron. *t-test* **P = 0.0013 (WT: 54.1 ± 7.7, N=3, n=9; W1989R: 19.8 ± 3.1, N=3, n=8). **(c)** Spontaneous inhibitory post-synaptic current (sIPSC) representative traces from CA1 hippocampal neurons in WT (black) and *Ank3* W1989R (red) slices. Scale bars: 200 pA, 1000 ms. **(d)** Quantification of spontaneous inhibitory post-synaptic current (sIPSC) frequency in CA1 hippocampal neurons WT (black circles) and *Ank3* W1989R (red squares) brain slices. *t-test* ***P = 0.0002 (WT: 4.7 ± 0.6 Hz, n=11; W1989R: 1.5 ± 0.3 Hz, n=10). **(e)** Quantification of sIPSC amplitude in WT (black circles) and *Ank3* W1989R (red squares) CA1 hippocampal neurons in brain slices. *t-test* ***P = 0.0027 (WT: 89.1 ± 10.1 pA, n=11; W1989R: 51.0 ± 3.3 pA, n=10). **(f)** Cumulative histogram of interspike interval frequency (black line) and *Ank3* W1989R (red line) CA1 hippocampal neurons using whole cell voltage-clamp recording. *t-test* ****P < 0.0001.

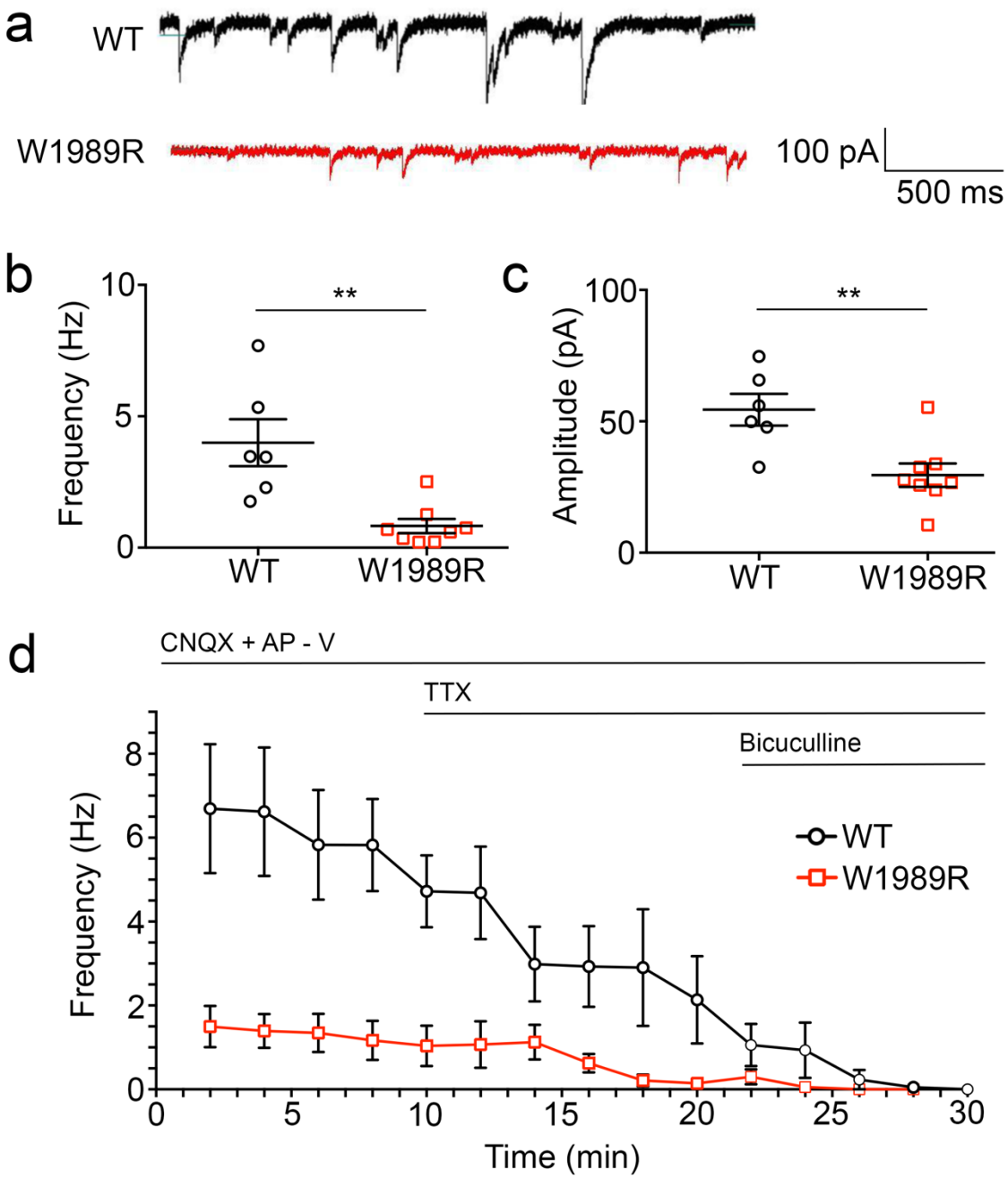
a
WT
W1989R
100 pA
500 ms
b
Frequency (Hz)
10
5
0
**
WT
W1989R
c
Amplitude (pA)
100
50
0
**
WT
W1989R
d
CNQX + AP - V
TTX
Bicuculline
WT
W1989R
Frequency (Hz)
8
6
4
2
0
0
5
10
15
20
25
30
Time (min)

Supplementary Fig. 4: Miniature inhibitory post-synaptic currents (mIPSCs) are decreased in *Ank3* W1989R cortical pyramidal neurons.

(a) Representative traces of miniature inhibitory post-synaptic currents (mIPSCs) of whole cell voltage-clamp recordings from layer II/III somatosensory cortical neurons in WT (black) and *Ank3* W1989R (red) homozygous brain slices. Scale bar: 100 pA, 500 ms. **(b)** Quantification of mIPSC frequency in WT (black circles) and *Ank3* W1989R homozygous (red squares) brain slices. *t-test* **P = 0.0023 (WT: 4.0 ± 0.9 Hz, n=6; W1989R: 0.83 ± 0.27 Hz, n=8). **(c)** Quantification of mIPSC amplitude in WT (black circles) and W1989R (red squares) brain slices. *t-test* **P = 0.0052 (WT: 54.4 ± 6.0 pA, n=6; W1989R: 29.5 ± 4.5 pA, n=8). **(d)** Quantification of IPSC frequency in response to tetrodotoxin (TTX) and bicuculline between WT (black circles) and *Ank3* W1989R homozygous (red squares).

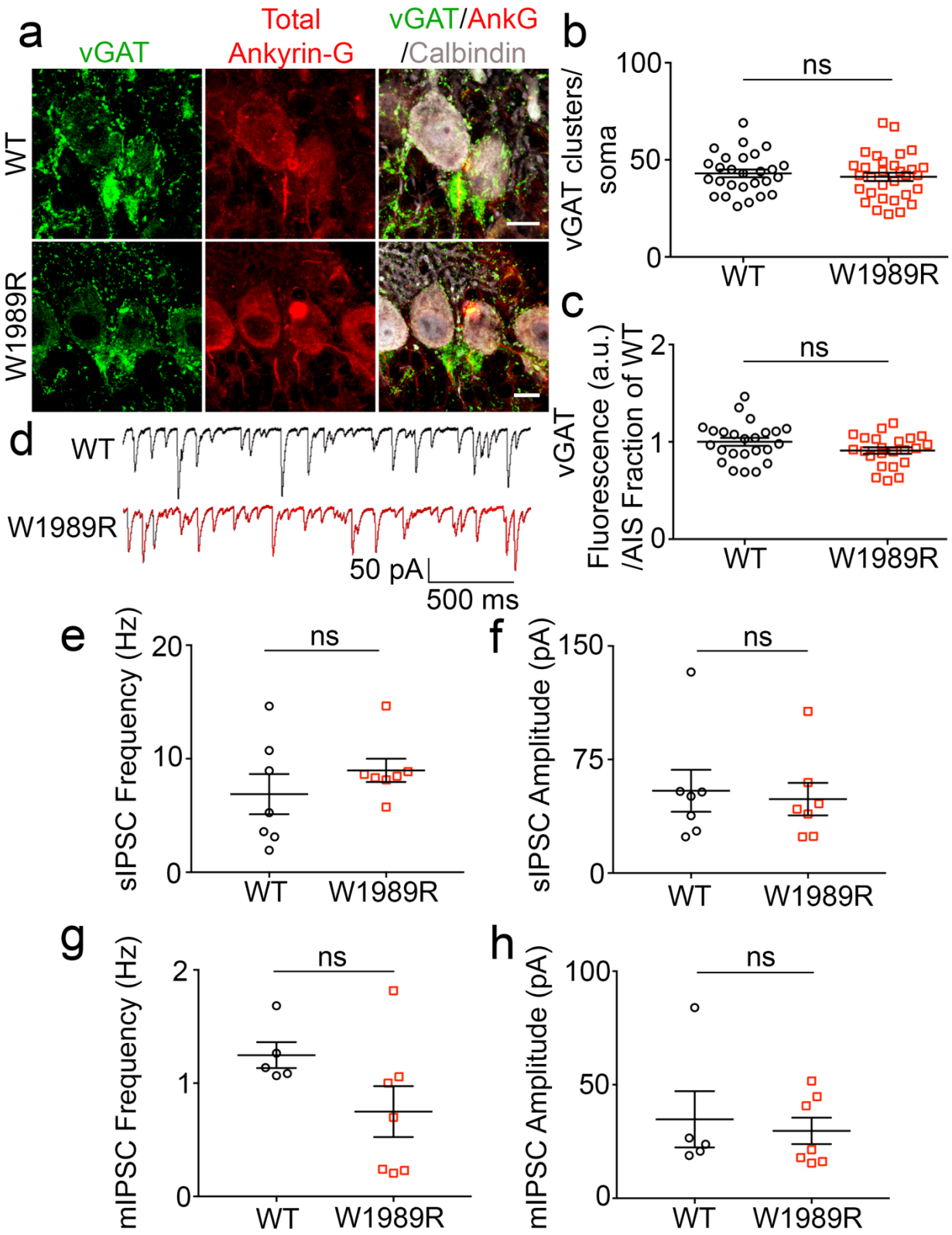
a
vGAT
Total
Ankyrin-G
vGAT/AnkG
/Calbindin
WT
W1989R
b
vGAT clusters/
soma
100
50
0
ns
WT
W1989R
c
vGAT
Fluorescence (a.u.)
/AIS Fraction of WT
2
1
0
ns
WT
W1989R
d
WT
W1989R
50 pA
500 ms
e
sIPSC Frequency (Hz)
20
10
0
ns
WT
W1989R
f
sIPSC Amplitude (pA)
150
75
0
ns
WT
W1989R
g
mIPSC Frequency (Hz)
2
1
0
ns
WT
W1989R
h
mIPSC Amplitude (pA)
100
50
0
ns
WT
W1989R

Supplementary Fig. 5: GABAergic synapses are maintained in the cerebellum of *Ank3* W1989R mice.

(a) Representative images of GABAergic synapses from cerebellar Purkinje neurons of P30 WT (top) and *Ank3* W1989R homozygous (bottom) mice. Sagittal brain sections immunostained for vGAT (green), total ankyrin-G (red), and calbindin (white). Scale bar: 10 µm. **(b)** Quantification of the total number of vGAT-positive clusters per soma above a set intensity threshold from WT (black circles) and *Ank3* W1989R homozygous (red squares) mice. *t-test* P = 0.54 (WT: 43.1 ± 2.0, N=3, n=27; W1989R: 41.3 ± 2.1, N=3, n=31). **(c)** Quantification of vGAT fluorescence intensity (a.u.) as fraction to WT between WT (black circles) and *Ank3* W1989R homozygous (red squares) mice. *t-test* P = 0.1 (WT: 1 ± 0.04, N=3, n=24; W1989R: 0.91 ± 0.03, N=3, n=23). **(d)** Spontaneous inhibitory post-synaptic current (sIPSC) representative traces from cerebellar Purkinje neurons in WT (black) and *Ank3* W1989R (red) slices. Scale bars: 50 pA, 500 ms. **(e)** Quantification of sIPSC frequency in WT (black circles) and *Ank3* W1989R (red squares) brain slices. *t-test* P = 0.33 (WT: 6.9 ± 1.8 Hz, n=7; W1989R: 8.9 ± 1.0 Hz, n=7). **(f)** Quantification of sIPSC amplitude in WT (black circles) and *Ank3* W1989R (red squares) brain slices. *t-test* P = 0.76 (WT: 54.4 ± 13.9 pA, n=7; W1989R: 48.8 ± 10.7 pA, n=7). **(g)** Quantification of mIPSC frequency in WT (black circles) and *Ank3* W1989R (red squares) brain slices. *t-test* P = 0.11 (WT: 1.23 ± 0.1 Hz, n=5; W1989R: 0.75 ± 0.2 Hz, n=7). **(h)** Quantification of mIPSC amplitude in WT (black circles) and *Ank3* W1989R (red squares) brain slices. *t-test* P = 0.69 (WT: 34.8 ± 12.4 pA, n=5; W1989R: 29.7 ± 5.8 pA, n=7).

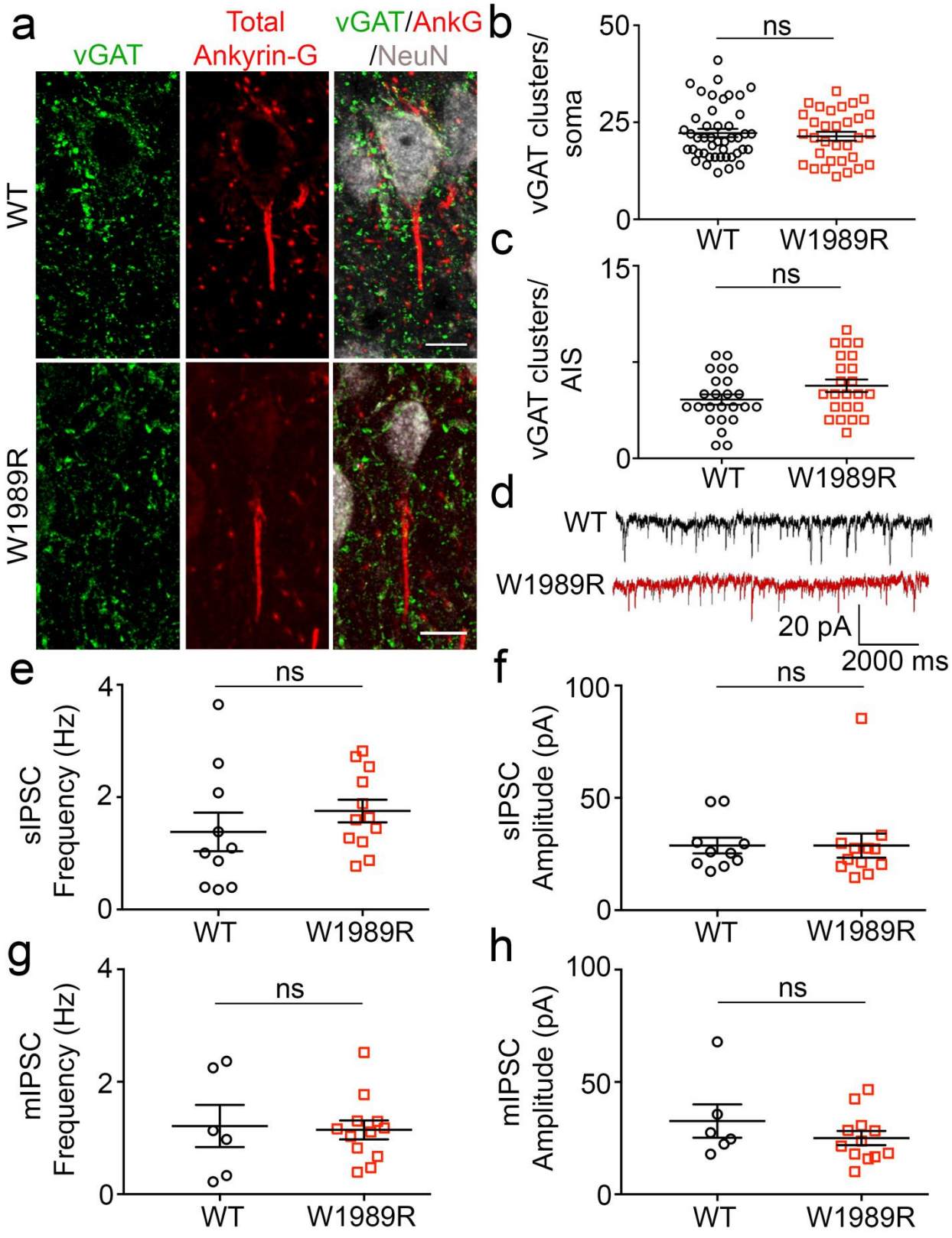
a
vGAT
Total Ankyrin-G
vGAT/AnkG /NeuN
WT
W1989R
b
vGAT clusters/ soma
50
25
0
ns
WT
W1989R
c
vGAT clusters/ AIS
15
0
ns
WT
W1989R
d
WT
W1989R
20 pA
2000 ms
e
sIPSC Frequency (Hz)
4
2
0
ns
WT
W1989R
f
sIPSC Amplitude (pA)
100
50
0
ns
WT
W1989R
g
mIPSC Frequency (Hz)
4
2
0
ns
WT
W1989R
h
mIPSC Amplitude (pA)
100
50
0
ns
WT
W1989R

Supplementary Fig. 6: Thalamic neurons display normal inhibitory currents in *Ank3* W1989R mice.

(a) Representative images of GABAergic synapses on thalamic neurons of P30 WT (top) and *Ank3* W1989R homozygous (bottom) mice. Coronal brain sections immunostained for vGAT (green), total ankyrin-G (red), and NeuN (white). Scale bar: 10 µm. **(b)** Quantification of the total number of vGAT-positive clusters per soma above a set intensity threshold from WT (black circles) and *Ank3* W1989R homozygous (red squares) mice. *t-test* P = 0.6 (WT: 22.2 ± 1.1, N=3, n=45; W1989R: 21.4 ± 1.2, N=3, n=32. **(c)** Quantification of total number of vGAT-positive clusters per AIS from WT (black circles) and *Ank3* W1989R homozygous (red squares) mice. *t-test* P = 0.09 (WT: 4.6 ± 0.4, N=3, n=24; W1989R: 5.7 ± 0.5, N=3, n=23). **(d)** Spontaneous inhibitory post-synaptic current (sIPSC) representative traces from thalamic neurons in WT (black) and *Ank3* W1989R (red) slices. Scale bars: 20 pA, 2000 ms. **(e)** Quantification of sIPSC frequency in WT (black circles) and *Ank3* W1989R (red squares) brain slices. *t-test* P = 0.34 (WT: 1.4 ± 0.3 Hz, n=10; W1989R: 1.8 ± 0.2 Hz, n=12). **(f)** Quantification of sIPSC amplitude in WT (black circles) and *Ank3* W1989R (red squares) brain slices. *t-test* P = 0.99 (WT: 28.8 ± 3.5 pA, n=10; W1989R: 28.8 ± 5.4 pA, n=12). **(g)** Quantification of mIPSC frequency in WT (black circles) and *Ank3* W1989R (red squares) brain slices. *t-test* P = 0.84 (WT: 1.2 ± 4 Hz, n=6; W1989R: 1.1 ± 0.2 Hz, n=12). **(h)** Quantification of mIPSC amplitude in WT (black circles) and *Ank3* W1989R (red squares) brain slices. *t-test* P = 0.28 (WT: 32.6 ± 7.4 pA, n=6; W1989R: 25.0 ± 3.2 pA, n=12).

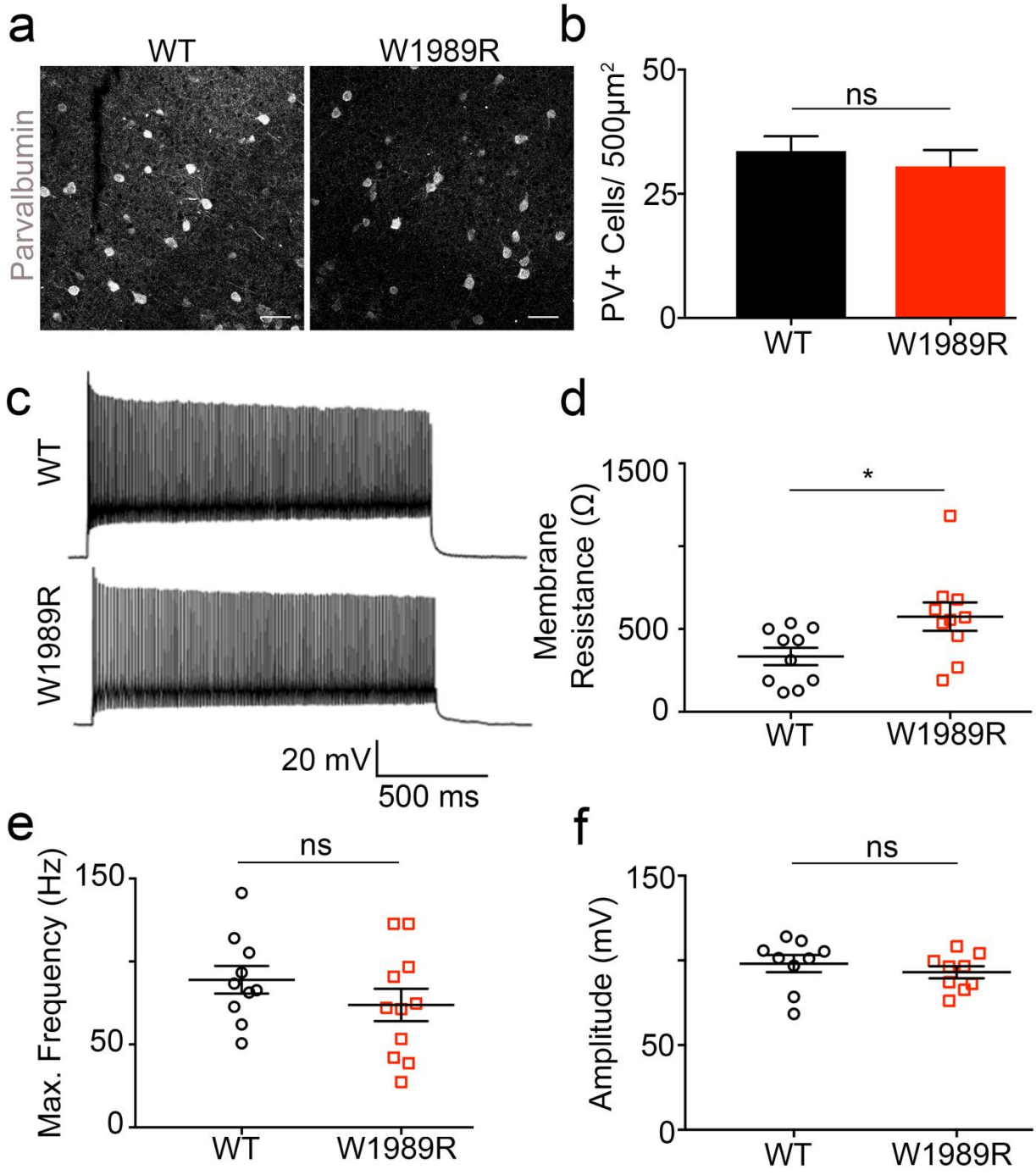
a
WT
W1989R
Parvalbumin
b
PV+ Cells/ 500µm²
50
25
0
ns
WT
W1989R
c
WT
W1989R
20 mV
500 ms
d
Membrane Resistance (Ω)
1500
500
0
*
WT
W1989R
e
Max. Frequency (Hz)
150
50
0
ns
WT
W1989R
f
Amplitude (mV)
150
50
0
ns
WT
W1989R

Supplementary Fig. 7*:* Normal density and fast-spiking properties of *Ank3* W1989R PV+ GABAergic interneurons.

(a) Representative images of parvalbumin-positive (PV+) interneurons in layer II/III somatosensory cortex of P30 WT (left) and *Ank3* W1989R homozygous (right) mice. Coronal brain sections immunostained with PV (white). Scale bar: 50 µm. **(b)** Quantification of total number of PV-positive cells per 500 μm^2 from WT (black bar) and *Ank3* W1989R homozygous (red bar) sections. *t-test* P = 0.497, ns, not significant (WT: 33.6 ± 3.0, N=3, n=15; W1989R: 30.5 ± 3.3, N=3, n=14). **(c)** Representative traces of evoked firing patterns and AP frequencies of fast-spiking PV+ interneurons in layer II/III somatosensory cortex from WT (top) and *Ank3* W1989R homozygous (bottom) brain slices. Scale bar: 20 mV, 500 ms. **(d)** Quantification of membrane resistance of PV+ cells in WT (black circles) and *Ank3* W1989R homozygous (red squares). *t-test* *P = 0.0276 (WT: 334.5 ± 52.8, n=10; W1989R: 574.9 ± 85.31, n=10). **(e)** Quantification of PV+ cell maximum frequency in WT (black circles) and *Ank3* W1989R homozygous (red squares). *t-test* P = 0.256 (WT: 89.0 ± 8.3, n=10; W1989R: 73.8 ± 9.7, n=11). **(f)** Quantification of single AP amplitude of PV+ in WT (black circles) and *Ank3* W1989R homozygous (red squares). *t-test* P = 0.422 (WT: 98.1 ± 5.0, n=9; W1989R: 93.0 ± 3.5, n=10). Data shown as mean ± SEM.

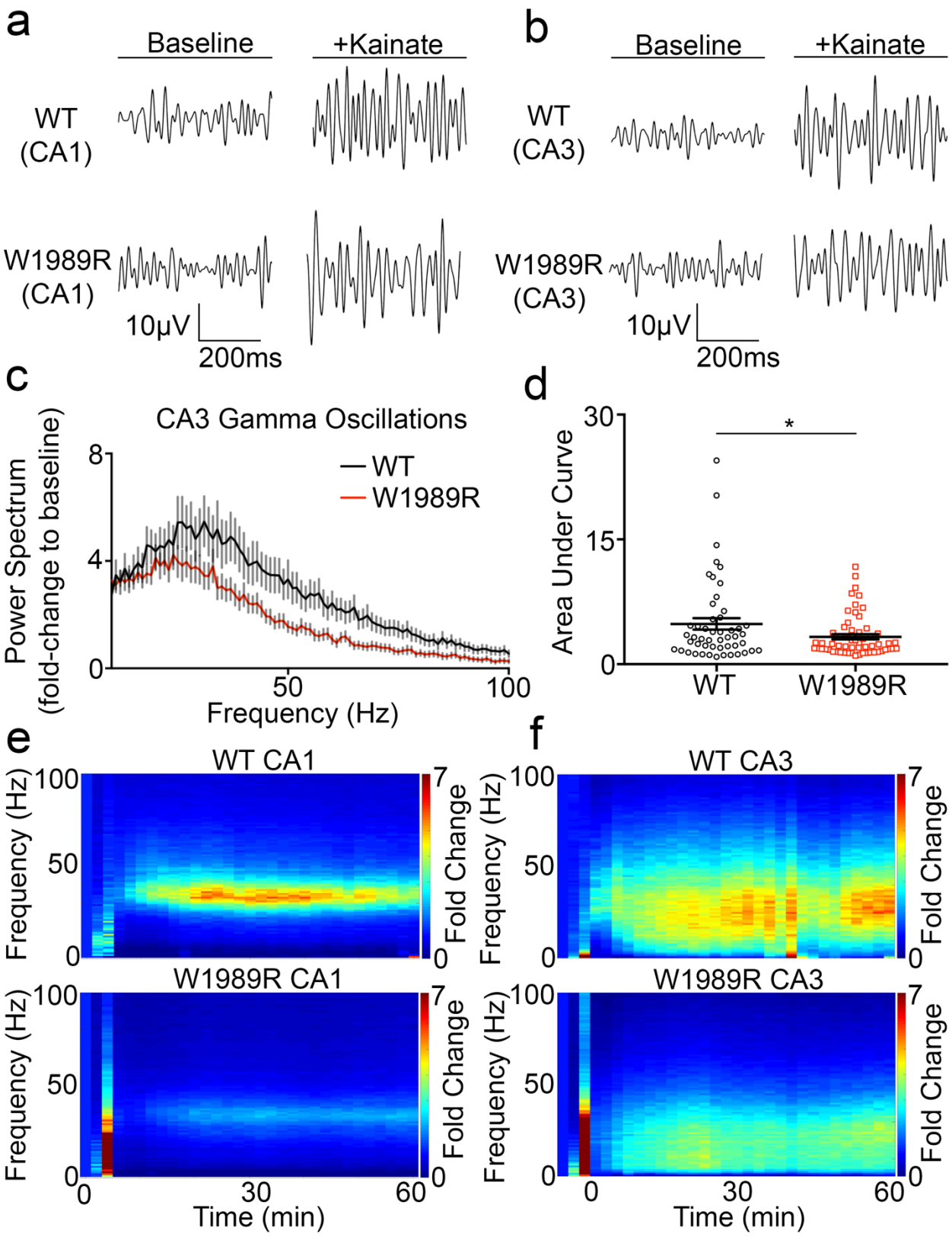
a
Baseline
+Kainate
WT
(CA1)
W1989R
(CA1)
10μV
200ms
b
Baseline
+Kainate
WT
(CA3)
W1989R
(CA3)
10μV
200ms
c
CA3 Gamma Oscillations
WT
W1989R
Power Spectrum
(fold-change to baseline)
Frequency (Hz)
d
Area Under Curve
*
WT
W1989R
e
WT CA1
W1989R CA1
Frequency (Hz)
Fold Change
Time (min)
f
WT CA3
W1989R CA3
Frequency (Hz)
Fold Change
Time (min)

Supplementary Fig. 8: Reduced gamma oscillations in the hippocampus of *Ank3* W1989R mice.

(a) Representative traces of kainate-induced gamma oscillations from local field potential (LFP) recordings in CA1 hippocampal neurons and **(b)** CA3 hippocampal neurons of WT (top) or *Ank3* W1989R homozygous (bottom) mice in acute brain slices. **(c)** Power spectral analysis from CA3 hippocampus WT (black circles) and *Ank3* W1989R homozygous (red squares) mice. **(d)** Quantification of the area under the curve for gamma band (30-60Hz) from WT (black circles) and *Ank3* W1989R homozygous (red squares). *t-test* *P=0.0343 (WT: 4.85 ± 0.7, N=5, n=50; W1989R: 3.3 ± 0.3, N=5, n=59). **(e)** Representative time-frequency sonograms of CA1 hippocampal neurons from WT (top) and W1989R homozygous (bottom) mice. **(f)** Representative time-frequency sonograms of CA3 hippocampal neurons from WT (top) and W1989R homozygous (bottom) mice.

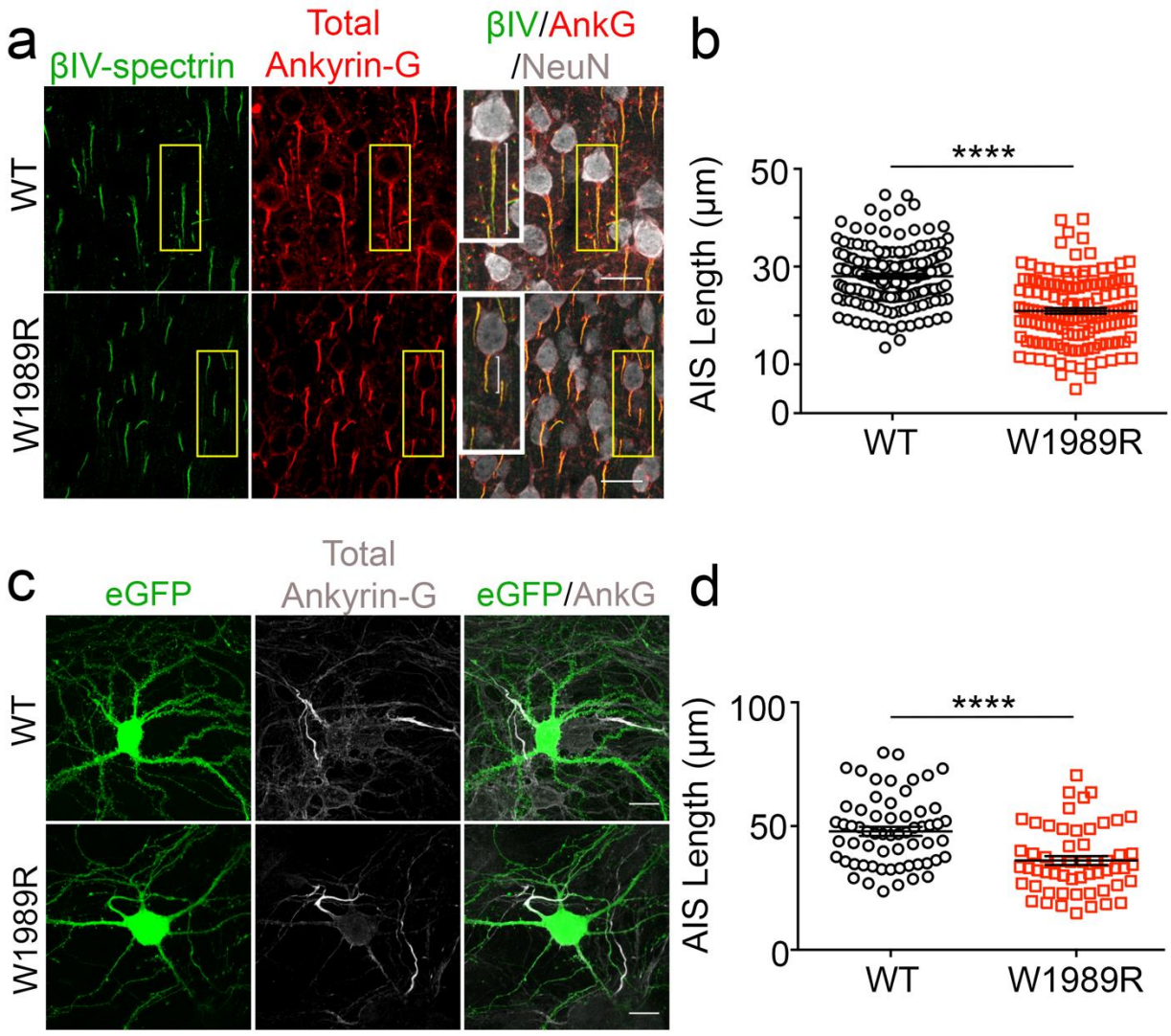
a
βIV-spectrin
Total
Ankyrin-G
βIV/AnkG
/NeuN
WT
W1989R
b
AIS Length (μm)
50
30
10
0
****
WT
W1989R
c
eGFP
Total
Ankyrin-G
eGFP/AnkG
WT
W1989R
d
AIS Length (μm)
100
50
0
****
WT
W1989R

Supplementary Fig. 9: Cortical and hippocampal pyramidal neurons have decreased AIS length in *Ank3* W1989R mice.

(a) Representative images from coronal sections of layer II/III somatosensory cortex of P30 WT (top) and *Ank3* W1989R homozygous (bottom) mice. Immunostaining for βIV-spectrin (green), total ankyrin-G (red), and NeuN (white). Scale bar: 20 µm. **(b)** Quantification of AIS length between WT (black circles) and W1989R homozygous (red squares) mice. *t-test* ****P < 0.0001 (WT: 28.03 ± 0.5, N=3, n=156; W1989R: 20.94 ± 0.6, N=3, n=140). **(c)** Representative images of dissociated hippocampal cultured neurons from WT (left) and *Ank3* W1989R homozygous (right) mice at 21DIV filled with soluble eGFP. Scale bar: 20 µm. **(d)** Quantification of the AIS length between WT (black circles) and *Ank3* W1989R homozygous (red squares) neurons. *t-test* ****P < 0.0001 (WT: 47.87 ± 1.8, N=3, n=61; W1989R: 36.11 ± 1.8, N=3, n=56).

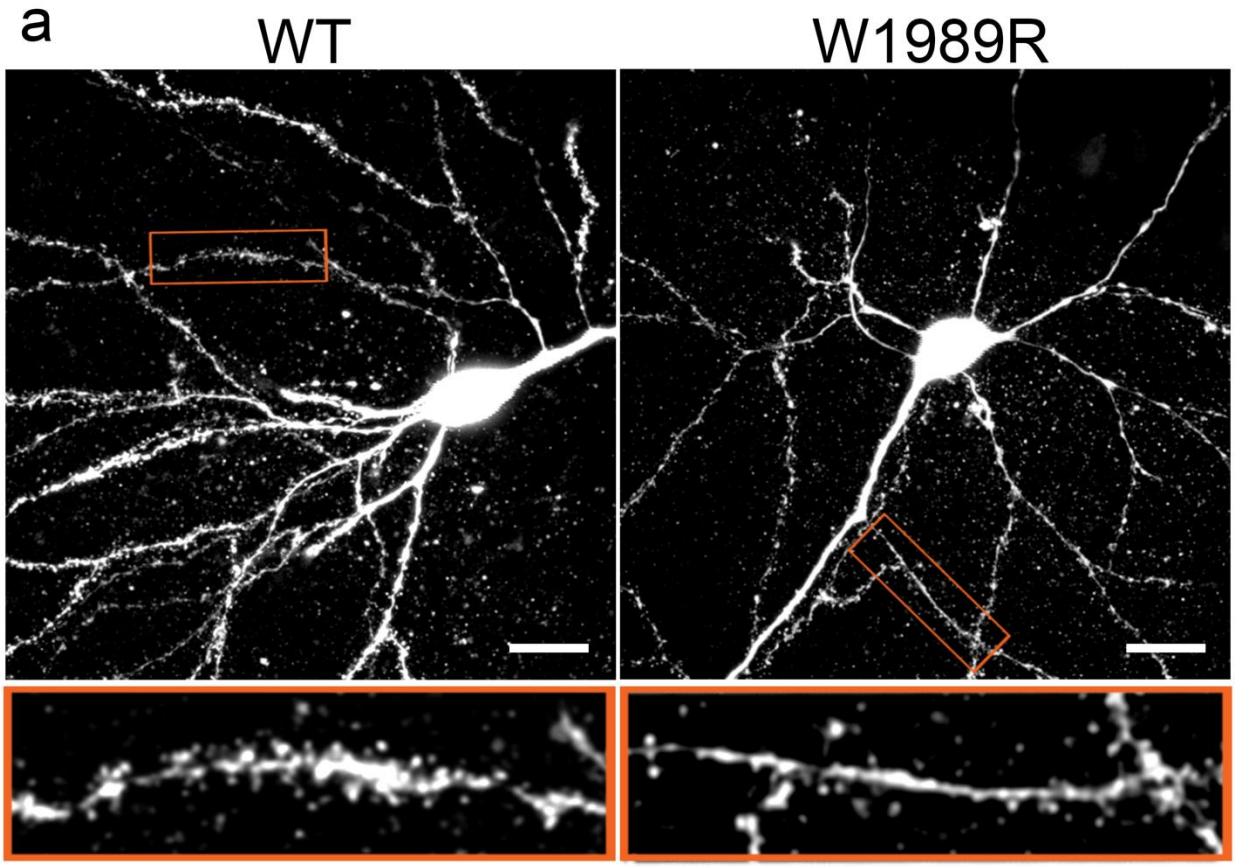
a
WT
W1989R

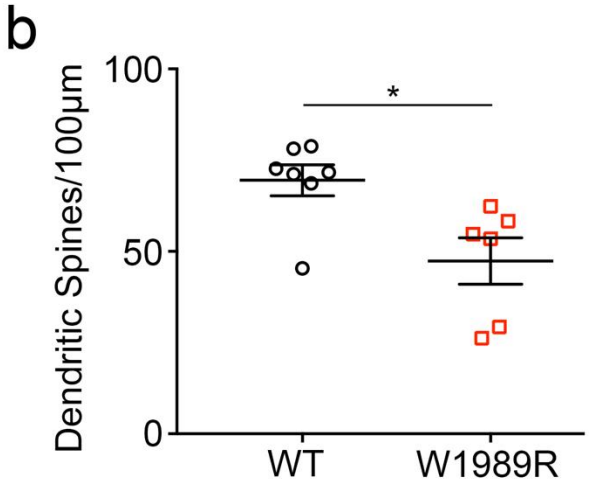
b
Dendritic Spines/100µm
100
50
0
*
WT
W1989R

Supplementary Fig. 10: Decreased dendritic spine density in CA1 hippocampal pyramidal neurons in *Ank3* W1989R mice *in vivo*.

(a) Representative images of biocytin-filled CA1 hippocampal pyramidal neurons of P30 WT (left) and *Ank3* W1989R homozygous (right) mice. Images were pseudocolored white. Scale bar: 20 µm. **(b)** Quantification of the number of dendritic spines per 100 µm of dendrite length in CA1 hippocampal pyramidal neurons. *t-test* *P < 0.01 (WT: 69.5 ± 4.3, N=3, n=7; W1989R: 47.4 ± 6.3, N=3, n=6).

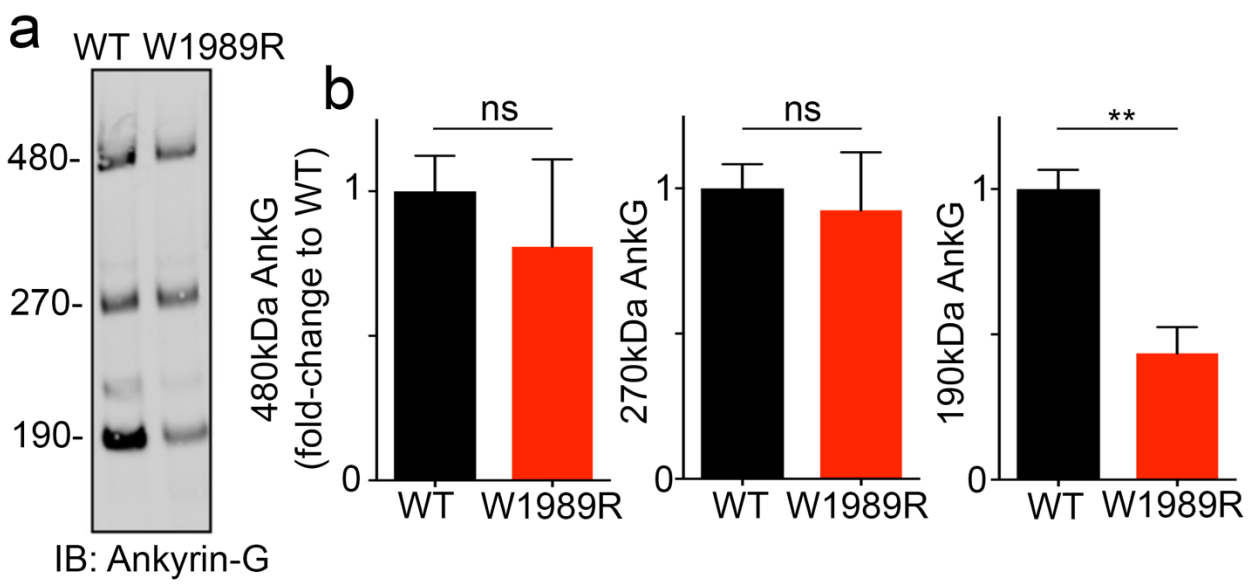

Supplementary Fig. 11: 190 kDa ankyrin-G expression levels are reduced in cortex of *Ank3* W1989R mice.

(a) Western blot analysis from cortical lysates of P30 WT (left) and *Ank3* W1989R homozygous (right) mice. Blots were probed with antibodies to total ankyrin-G. **(b)** Quantification of relative expression levels of 480 kDa ankyrin-G *t-test* P = 0.59 (WT: 1.0 ± 0.1, N=3; W1989R: 0.81 ± 0.3, N=3), 270 kDa ankyrin-G *t-test* P = 0.75 (WT: 1.0 ± 0.1, N=3; W1989R: 0.92 ± 0.2, N=3), and 190 kDa ankyrin-G *t-test* **P = 0.0073 (WT: 1 ± 0.1 N=3; W1989R: 0.43 ± 0.1, N=3). Data normalized to WT controls. Data shown as mean ± SEM.

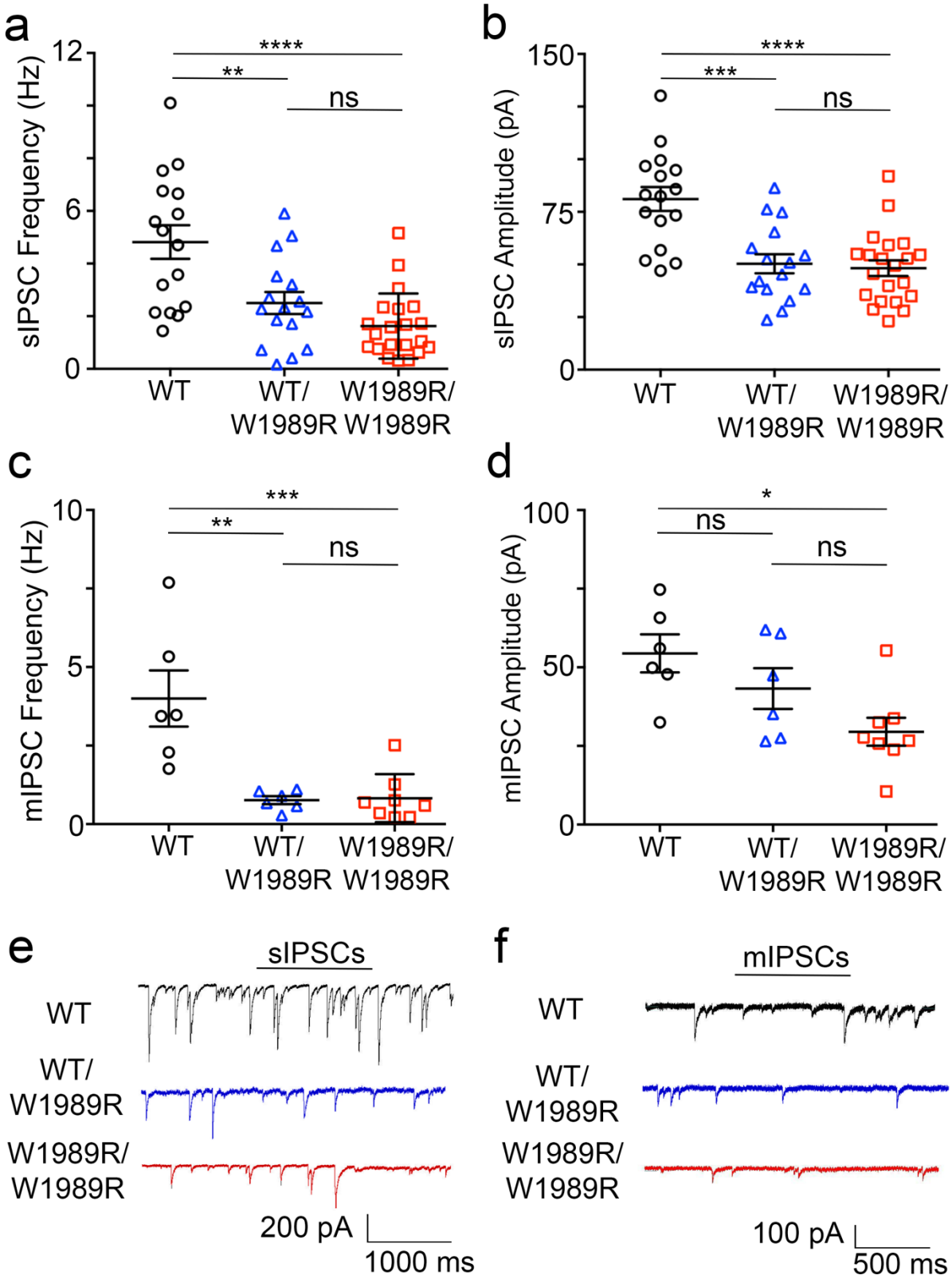
a
sIPSC Frequency (Hz)
12
6
0
****
**
ns
WT
WT/ W1989R
W1989R/ W1989R
b
sIPSC Amplitude (pA)
150
75
0
****
***
ns
WT
WT/ W1989R
W1989R/ W1989R
c
mIPSC Frequency (Hz)
10
5
0
***
**
ns
WT
WT/ W1989R
W1989R/ W1989R
d
mIPSC Amplitude (pA)
100
50
0
*
ns
ns
WT
WT/ W1989R
W1989R/ W1989R
e
sIPSCs
WT
WT/ W1989R
W1989R/ W1989R
200 pA
1000 ms
f
mIPSCs
WT
WT/ W1989R
W1989R/ W1989R
100 pA
500 ms

Supplementary Fig. 12: Heterozygous *Ank3* W1989R mice have reduced GABAergic synapse function.

Comparison of P25-48 heterozygous *Ank3* W1989R mice to wild-type and homozygous *Ank3* W1989R mice. Note: wild-type and *Ank3* W1989R homozygous mouse data are from Fig. 2 and Supplemental Fig. 4 and shown for comparison purposes. **(a)** Quantification of sIPSC frequency in WT (black circles), heterozygous *Ank3* WT/W1989R (blue triangles), and homozygous *Ank3* W1989R/W1989R (red squares) brain slices. *One-way ANOVA, Tukey's post hoc.* WT vs. WT/W1989R **P = 0.0023, WT vs. W1989R/W1989R ****P < 0.0001, WT/W1989R vs. W1989R/W1989R P = 0.33 (WT: n=16; WT/W1989R: n=16; W1989R/W1989R n=21). **(b)** Quantification of sIPSC amplitude in WT (black circles), heterozygous *Ank3* WT/W1989R (blue triangles), and homozygous *Ank3* W1989R/W1989R (red squares) slices. *One-way ANOVA, Tukey's post hoc.* WT vs. WT/W1989R ***P = 0.0001, WT vs. W1989R/W1989R ****P < 0.0001, WT/W1989R vs. W1989R/W1989R P = 0.94 (WT: n=16; WT/W1989R: n=16; W1989R/W1989R n=21). **(c)** Quantification of mIPSC frequency in WT (black circles), heterozygous *Ank3* WT/W1989R (blue triangles), and homozygous *Ank3* W1989R/W1989R (red squares) slices. *One-way ANOVA, Tukey's post hoc.* WT vs. WT/W1989R **P = 0.001, WT vs. W1989R/W1989R ***P = 0.0008, WT/W1989R vs. W1989R/W1989R P = 0.99 (WT: n=6; WT/W1989R: n=6; W1989R/W1989R n=8). **(d)** Quantification of mIPSC amplitude in WT (black circles), heterozygous *Ank3* WT/W1989R (blue triangles), and homozygous *Ank3* W1989R/W1989R (red squares) slices. *One-way ANOVA, Tukey's post hoc.* WT vs. WT/W1989R P = 0.38, WT vs. W1989R/W1989R *P = 0.01, WT/W1989R vs. W1989R/W1989R P = 0.21 (WT: n=6;

WT/W1989R: n=6; W1989R/W1989R n=8). **(e)** Representative traces of spontaneous inhibitory post-synaptic currents (sIPSCs) of layer II/III somatosensory cortical neurons in WT (black circles), heterozygous *Ank3* WT/W1989R (blue triangles), and homozygous *Ank3* W1989R/W1989R (red squares) slices. Scale bars: 200 pA, 1000 ms. **(f)** Representative traces of miniature inhibitory post-synaptic currents (mIPSCs) from layer II/III somatosensory cortical neurons in WT (black), and *Ank3* W1989R (red) homozygous brain slices. Scale bar: 100 pA, 500 ms.

Table 1: Statistics of X-ray Crystallographic Data Collection and Model Refinement

Data Collection:

Data sets	Ankyrin-G/ GABARAP
Space group	I23
Wave length (Å)	0.9785
Unit Cell Parameters	a=b=c=96.99 a=b=γ=90°
Resolution range (Å)	50-2.20 *2.24-2.20)
No. of unique reflections	7843 (367)
Redundancy	20.0 (19.6)
I/σ	45.2 (2.6)
Completeness (%)	99.9 (100)
R_{merge} [a] (%)	6.9 (>100)
$CC_{1/2}$ (last resolution shell)[b]	0.792
Structure refinement:	
Resolution (Å)	50-2.20 (2.77-2.20)
R_{crvst} [c]/R_{free} [d] (%)	20.27/24.89 (25.57/30.84)
rmsd bonds (Å) / angles (°)	0.006 / 0.93
Average B factor (Å^2) [e]	34.2
No. of atoms	
Protein atoms	1087
Water	15
No. of reflections	
Working set	7396 (3611)
Test set	349 (174)
Ramachandran plot regions	
Favored (%)	98.5
Allowed (%)	1.5
Outliers (%)	0

Table 1: Statistics of x-ray crystallographic data collection and model refinement.

Summary statistics of X-ray crystallography data from the crystal structures in Fig. 1 and Supplemental Fig. 1.

Table 2: Cell-Type Electrophysiological Properties between WT and *Ank3* W1989R mice

		Membrane Resistance (MΩ)	Membrane Potential (mV)	AP Threshold (mV)	AP Amplitude (mV)	AP Peak Time (ms)	AP Width (ms)	AP Tau (ms)
Pyramidal	WT	228.3 ± 121 (n=27)	-67.5 ± 4 (n=22)	-40.7 ± 20 (n=22)	113.7 ± 13 (n=22)	2.6 ± 0.5 (n=22)	2.6 ± 0.6 (n=22)	25 ± 10 (n=22)
	W1989R	159.9 ± 66* (n=33)	-66.3 ± 5 (n=29)	-36.1 ± 30 (n=29)	111 ± 14 (n=29)	2.7 ± 1 (n=29)	2.8 ± 1 (n=29)	21.6 ± 10 (n=25)
Fast-Spiking	WT	334.6 ± 167 (n=10)	-62.1 ± 5 (n=9)	-46.3 ± 2 (n=9)	98.1 ± 15 (n=9)	2.1 ± 0.4 (n=9)	0.8 ± 0.1 (n=9)	0.9 ± 0.3 (n=9)
	W1989R	574.3 ± 269* (n=9)	-61.6 ± 6 (n=9)	-46.3 ± 2 (n=9)	93 ± 11 (n=9)	2.2 ± 0.4 (n=9)	1.0 ± 0.4 (n=9)	1.2 ± 0.8 (n=9)
Regular Spiking Nonpyramidal	WT	363.9 ± 108 (n=13)	-64.8 ± 5 (n=13)	-41 ± 10 (n=9)	110.2 ± 9 (n=9)	2.4 ± 0.2 (n=13)	2.5 ± 0.7 (n=13)	17.5 ± 11 (n=13)
	W1989R	284.3 ± 125 (n=17)	-57.5 ± 28 (n=18)	-47 ± 6* (n=18)	101.4 ± 15 (n=18)	2.6 ± 0.9 (n=18)	2.4 ± 0.2 (n=18)	12.4 ± 11 (n=17)
Irregular Spiking	WT	227.03 (n=1)	-60.9 ± 5 (n=3)	-43.9 ± 2 (n=3)	88.3 ± 5.6 (n=3)	3.1 ± 0.4 (n=3)	3.0 ± 0.5 (n=3)	9.5 ± 0.7 (n=3)
	W1989R	156.2 ± 14 (n=4)	-64.2 ± 4 (n=4)	-49.4 ± 1* (n=4)	107.4 ± 12 (n=4)	2.7 ± 0.2 (n=4)	3.1 ± 0.3 (n=4)	9.1 ± 1 (n=4)

Table 2: Comparison of cell-type specific electrophysiological properties between WT and *Ank3* W1989R mice. Quantification of various electrophysiology measurements of layer II/III cortical pyramidal neurons and the main classes of inhibitory interneurons following evoked APs in acute brain slices from WT and *Ank3* W1989R homozygous mice. Yellow/asterisk indicates significantly different from WT.

Table 3: Cell-type specific morphological and functional changes in *Ank3* W1989R mice

	vGAT (+) GABAergic Synapses	Inhibitory Post-synaptic Currents	Action Potential Firing Rate	Dendritic Spine Density	AIS Length
Layer II/III Somatosensory Cortical Pyramidal Neurons	↓	↓	↑	N.D.	↓
CA1 Hippocampal Pyramidal Neurons	↓	↓	↑	↓	↓
Thalamic Neurons	—	—	N.D.	N.D.	—
Cerebellar Purkinje Neurons	—	—	N.D.	N.D.	—

Table 3: Summary of cell-type specific morphological and functional differences in *Ank3* W1989R mice compared to WT. Summary of results demonstrating differences in GABAergic synapse number, GABA-mediated currents, action potential firing rate, dendritic spine density, and AIS length of layer II/III cortical and hippocampal pyramidal neurons, thalamic neurons, and cerebellar Purkinje neurons in *Ank3* W1989R mice compared to WT mice. Blue arrows indicate significantly decreased from WT, red arrows indicate significantly increased from WT, black lines indicate no difference from WT. N.D. represents not determined.